Extreme Precipitation Pathway Detection Algorithm using Multi-dimensional Climate Network

Reza Nosratpour[a,*], Laleh Tafakori[a], Mali Abdollahian[a]

[a] *School of Science, Engineering, and Health, Department of Mathematical Sciences, RMIT University, Melbourne, Australia*

Keywords: Extreme Precipitation Pathway Detection Algorithm using Tail Dependence Coefficient and K-means++ Clustering

Supplementary materials

Figure S1 presents the spatial distribution of the evaluation metrics. Overall, the results indicate larger errors along the east coast and in northern Australia; however, Spearman's correlation is also higher in these regions, suggesting a stronger monotonic relationship between IMERG precipitation estimates and gauge observations. The tail dependence coefficient likewise indicates stronger dependence between IMERG and observed precipitation in these areas, reaching values of up to 0.6, while the extremal correlation is particularly pronounced over the northern part of the Northern Territory. These findings suggest that IMERG performs effectively for near-real-time precipitation estimation, especially in northern Australia, along the east coast, and in southern Victoria under high precipitation thresholds.

Moreover, the MBE ranges from approximately -12 to 12 mm, indicating stronger underestimation over the east coast and the northern part of the Northern Territory. The RMSE (about 30–40 mm) and MAE (about 10–15 mm) are also relatively high in these regions, supporting the MBE results. In contrast, Spearman's correlation is around 0.20 in Western Australia, indicating comparatively weak performance of the IMERG dataset in this region. This is further supported by the values of $\theta \approx 1.6$ and $\chi_X \approx$ 0–0.2 in Western Australia, which suggest limited skill of IMERG in capturing extreme precipitation there.

This supplementary section includes further analyses and maps that enrich the understanding of the primary results and conclusions discussed in the main text.

Table 1 summarizes the execution times of each task within the proposed algorithm, evaluated using the RACE supercomputer. The results indicate that the majority of computation time is devoted to constructing the tail-dependence structure, particularly the graph-building and chain exploration phases, whereas the prediction stage executes rapidly. This efficiency suggests that the model is well-suited for early-warning

*Corresponding author. Email: `Rezanosratpour@rmit.edu.au`

Email addresses: `Rezanosratpour@hotmail.com` (Reza Nosratpour), `laleh.tafakori@rmit.edu.au` (Laleh Tafakori), `mali.abdollahian@rmit.edu.au` (Mali Abdollahian)

applications in extreme weather scenarios.

Figures S2 and S3 present the variance of the tail-dependence coefficient across different lead–lag configurations. A near-zero variance implies that the random combinations generated in Step 4: Chain Exploration yield consistent outcomes. Additionally, the variance reflects the degree of uncertainty associated with the estimated tail-dependence coefficients.

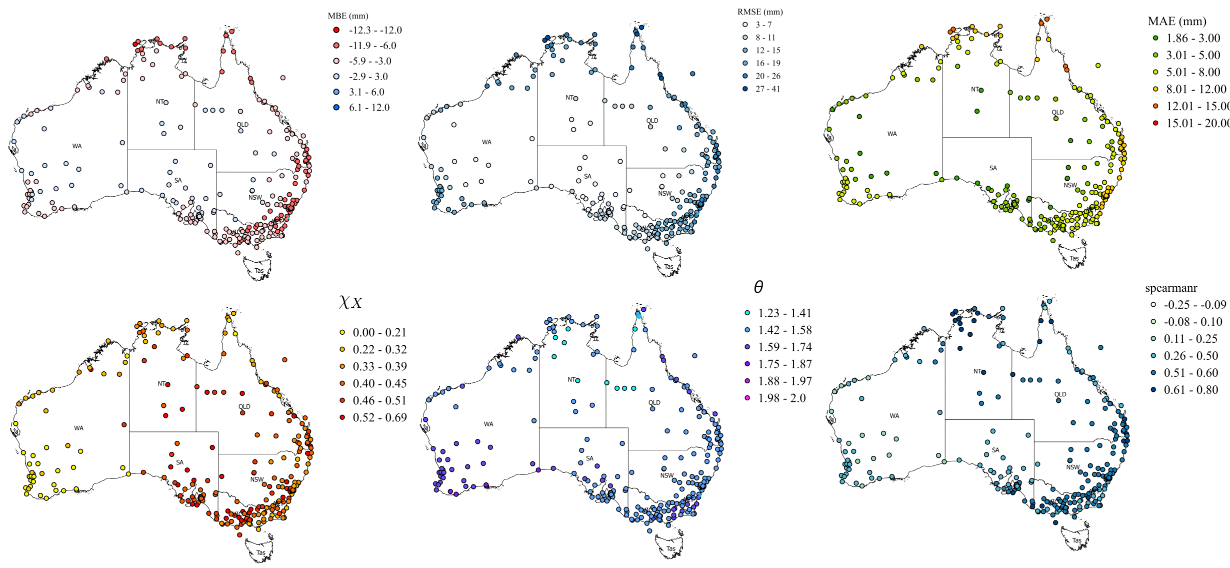

Figure S1: The Error Analysis of IMERG precipitation Dataset against the gauge precipitation observations from 2020 to 2023

Table 1: Processing time of the proposed algorithm tasks using the RACE supercomputer.

Task	**Processing time (seconds)**
Initializing the model	3.9
Constructing the Graph of Tail Dependence	62.7
Extreme Precipitation pathway	0.13
Clustering ($k = 2$ to 25)	6.74
Chain Exploration ($d = 3$)	73.5
Station-based chain exploration	124
Prediction of precipitation for each station	0.0004

Figure S4 shows the calculated χ_X for percentiles from 0.85 to 0.99 and combinations in $d = 3$ of time lags for different stations used in this study. The result show that χ_X decays with both increasing the time lags and percentiles. Based on the results of this study the asymptomatic independence has been shown for the southern part of Australia.

As explained in section 3.1 of methodology, under the asymptomatic independence a more useful information is the residual tail dependence parameter η_X. Figure S5 shows the maps of the residual tail dependence parameter η_X, for different time lags utilizing gauge precipitation observations from 2020 to 2023. Since η_X is higher than 0.5 a positive extermal association can interpreted for most of the the station. Moreover, the positive extermal association decays when the time lags increases to $[2, 2]$.

The results of this study have shown that the proposed algorithm is fast and accurate to detect the sources of extreme precipitation event for different regions across a continental case of study with diverse sources of extreme precipitation. In addition the initial stage of prediction can be used to develop an early warning precipitation estimation as the processing time is a fraction of second.

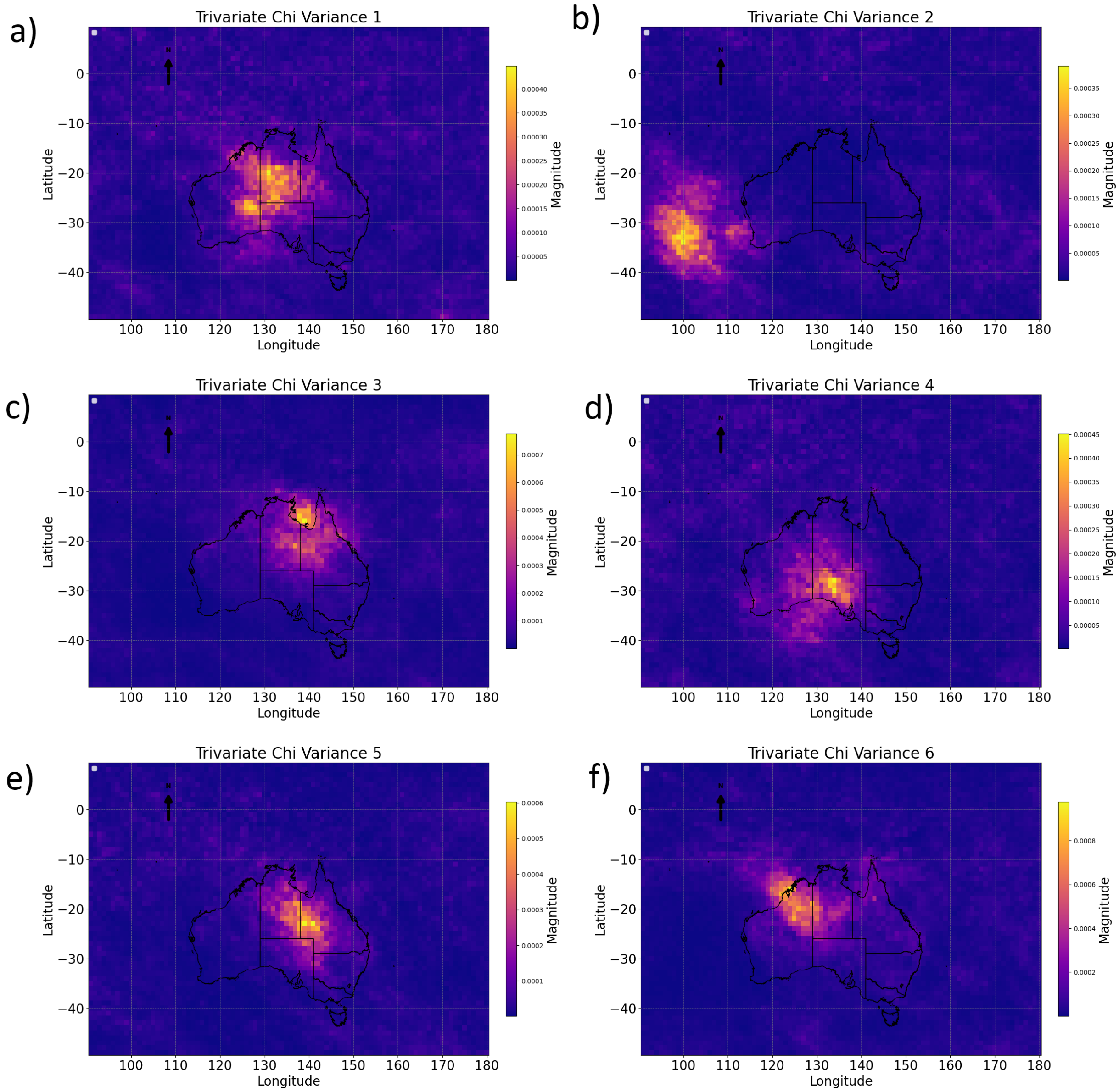

Figure S2: The tail dependence coeffient variance calculated by the propoesed algorithm with D=3, and time lags = [1,1], for different clusters from 2000 to 2019.

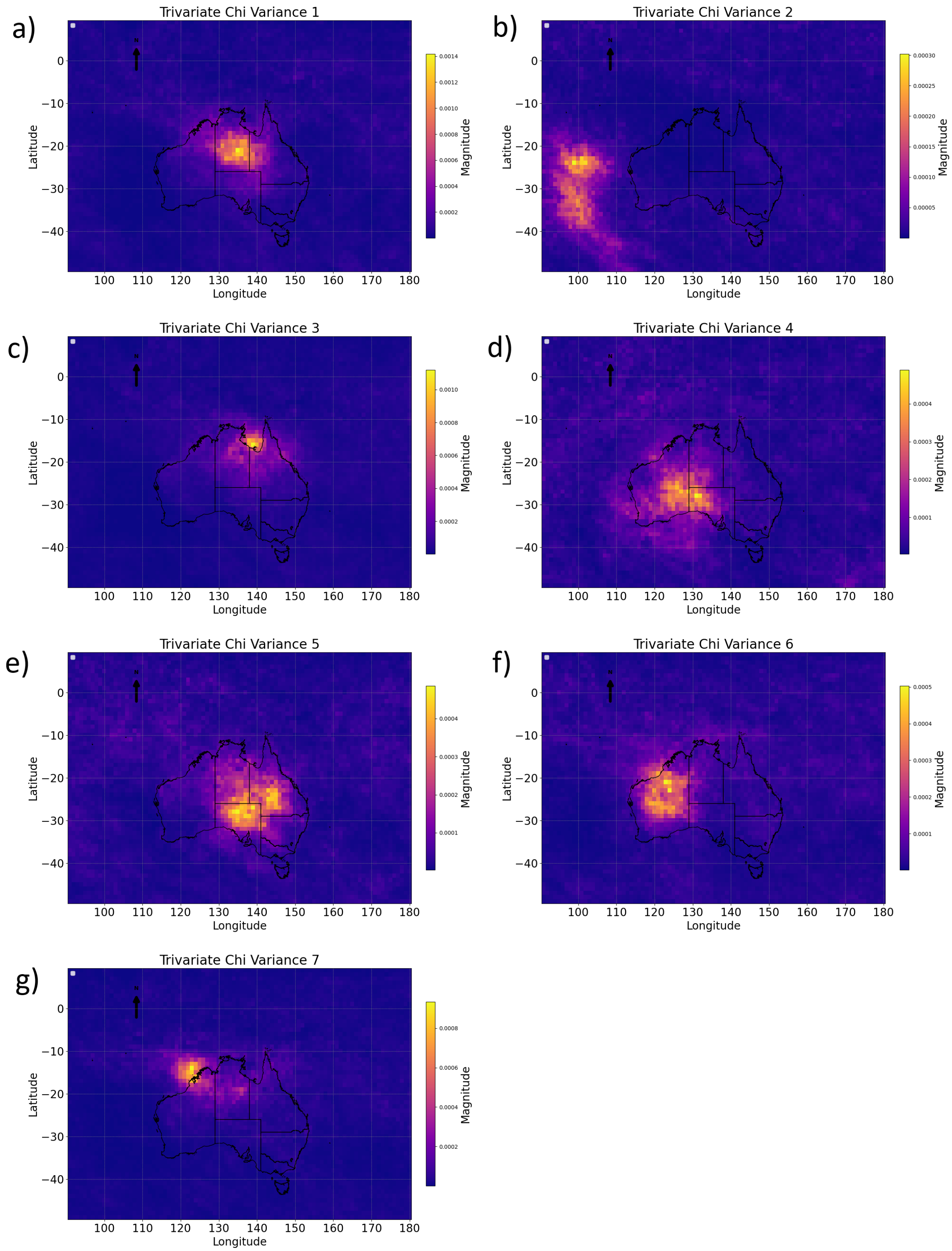

Figure S3: The tail dependence coeffient variance calculated by the propoesed algorithm with D=3, and time lags = [2,1], for different clusters from 2000 to 2019.

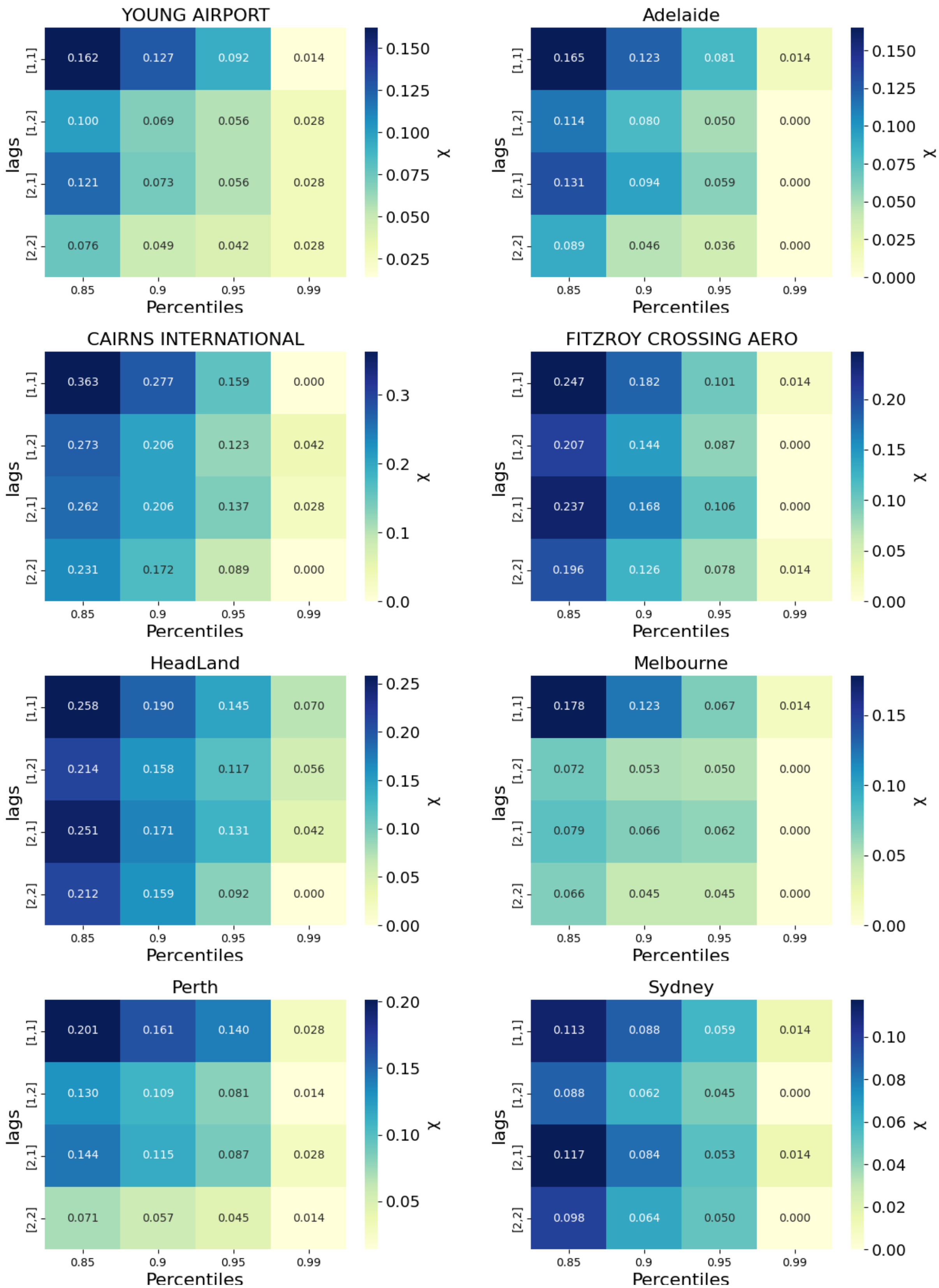

Figure S4: Tail dependence coefficient χ_X for different station with different combinations of time lags, and percentiles

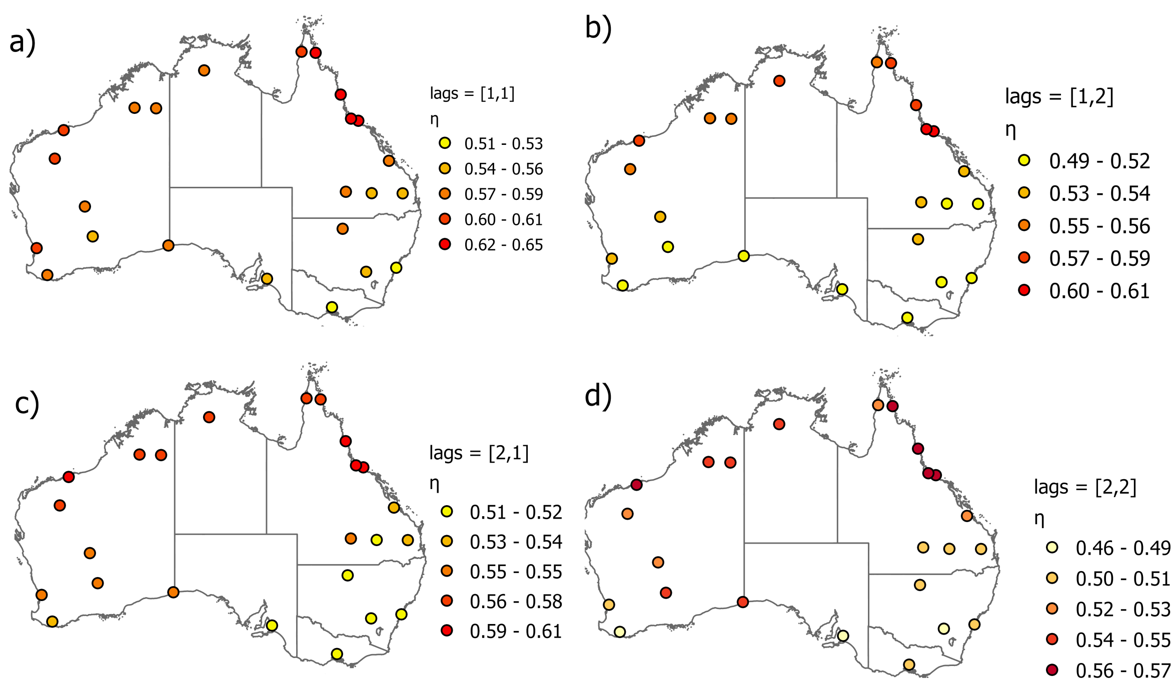

Figure S5: The maps of the residual tail dependence parameter η_X, for different time lags utilizing gauge precipitation observations from 2020 to 2023.